J Biomol NMR (2010) 47:237–241
DOI 10.1007/s10858-010-9420-1

NMR STRUCTURE NOTE

The NMR structure of the autophagy-related protein Atg8

Hiroyuki Kumeta · Masahiro Watanabe · Hitoshi Nakatogawa · Masaya Yamaguchi · Kenji Ogura · Wakana Adachi · Yuko Fujioka · Nobuo N. Noda · Yoshinori Ohsumi · Fuyuhiko Inagaki

Received: 16 February 2010 / Accepted: 8 April 2010 / Published online: 29 April 2010

Biological context

Autophagy is the process through which the bulk degradation of cytoplasmic components by the lysosomal/vacuolar system occurs in response to starvation conditions (Nakatogawa et al. 2009). In autophagy, a double-membrane structure called an autophagosome sequesters a portion of the cytoplasm and fuses with the lysosome/vacuole to deliver its contents into the organelle lumen. Recently, autophagy was found to have a crucial function in numerous biological processes including differentiation, antigen presentation and aging, and its dysfunction causes severe diseases such as neurodegeneration (Mizushima 2007).

Atg8 is a ubiquitin like protein, and plays an essential role for autophagosome formation in *Saccharomyces cerevisiae*. Atg8 is unique in that it is conjugated to the lipid phosphatidylethanolamine (PE) by a ubiquitin-like system, called the Atg8 system. In the Atg8 system, nascent Atg8 is cleaved at its C-terminal arginine residue by Atg4, a cysteine protease (Kirisako et al. 2000), and the exposed C-terminal glycine is conjugated to PE by Atg7, an E1-like enzyme and Atg3, an E2-like enzyme. The Atg8-PE conjugate itself possesses membrane tethering and hemifusion ability and is essential in autophagosome formation, especially in a membrane expansion step (Nakatogawa et al. 2007). It was also known that Atg8 plays a critical role for target recognition in selective autophagy. For example, aminopeptidase I (Ape1) is selectively and constitutively transported into the vacuole through autophagic processes. During these processes, Ape1 is recognized by the receptor protein Atg19, which is further recognized by Atg8. These interactions may facilitate biogenesis of autophagosomal membranes around Ape1 and selective sequestration of the enzyme into the membranes (Nakatogawa et al. 2009).

Structures of several Atg8 homologues have been determined (LC3; Sugawara et al. 2004, GABARAP; Bavro et al. 2002, Stangler et al. 2002, GATE-16; Paz et al. 2000, *Trypanosoma brucei* Atg8; Koopmann et al. 2009; reviewed by Noda et al. 2009). All of these homologues are comprised of two domains, an N-terminal α-helix domain and a C-terminal ubiquitin-like domain. However, *S. cerevisiae* Atg8 structure was only solved in the complex with the Atg19 peptide (Noda et al. 2008). Atg8 is suggested to take both an open and a closed conformations. The membrane biogenesis in autophagy is considered to be mediated through the open conformation that is oligomerized to initiate membrane fusion (Nakatogawa et al. 2007). This prompted us to study the structure of Atg8 at the peptide-free state.

The assignment of Atg8 NMR signals was reported by Schwarten et al. (2009). We also determined the main chain signal assignment at both ligand-free and ligand-bound states (Noda et al. 2008). However, NMR signals of the N-terminal region and Arg47 of Atg8 at a ligand-free state were very weak or not detectable. Furthermore, Atg8 at the

H. Kumeta · M. Watanabe · M. Yamaguchi · K. Ogura · W. Adachi · Y. Fujioka · N. N. Noda · F. Inagaki (✉)
Laboratory of Structural Biology, Graduate School of Pharmaceutical Sciences, Hokkaido University, Kita 12 Nishi 6, Kita-ku, Sapporo 060-0812, Japan
e-mail: finagaki@pharm.hokudai.ac.jp

H. Nakatogawa · Y. Ohsumi
Integrated Research Institute, Tokyo Institute of Technology, Yokohama 226-8503, Japan

H. Nakatogawa
PRESTO, Japan Science and Technology Agency, Saitama 332-0012, Japan

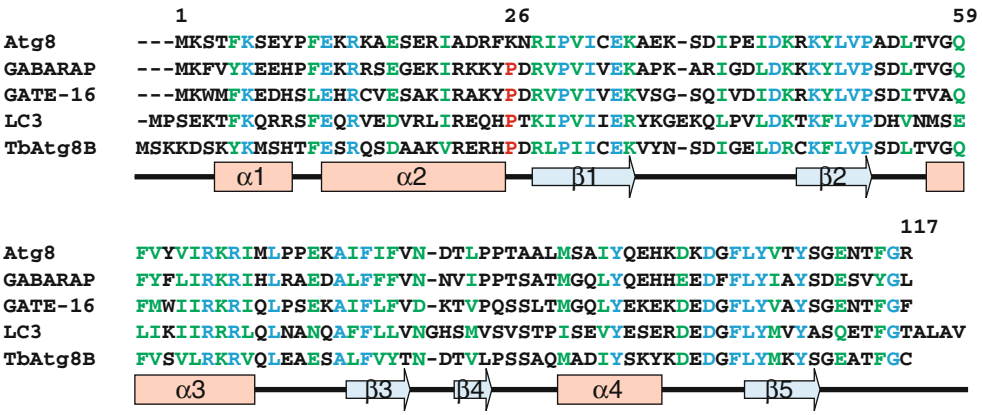

Fig. 1 Structure based sequence alignment of Atg8 and its homologues, GABARAP, GATE-16, LC3, and TbAtg8. The completely conserved residues in the Atg8 family are marked in *blue*, while type conserved residues are marked in *green*. The Pro26 conserved in Atg8 homologues but not in Atg8 is marked in *red*. The secondary structure is shown at the *bottom*

ligand-free state was aggregated at NMR sample conditions within 1 week and was not suitable for the NMR experiments. Thus, we constructed a mutant that is not aggregated at NMR conditions during NMR measurement but retains similar autophagic activity. Intriguingly, mammalian Atg8 homologues, especially LC3, were not aggregated even at higher concentration. Based on the sequential alignment of Atg8 with its homologues (Fig. 1), we constructed an Atg8 K26P mutant (Lys26 was replaced by Pro) that was found to be stable for over 1 month at NMR conditions. Here, we report the structure of Atg8 K26P at the ligand-free state.

Materials and methods

Protein expression and purification

The expression and purification procedures of Atg8 have been previously described (Yamada et al. 2007). An expression vector for the Atg8 mutant with an amino acid substitution from Lys26 to Pro (Atg8 K26P) was prepared by using a QuikChange site-directed mutagenesis kit (Stratagene). ^{15}N- or ^{13}C-/^{15}N- labeled protein was prepared by culturing *Escherichia coli* BL21 cells in M9 medium using $^{15}NH_4Cl$ and ^{13}C-glucose as sole nitrogen and carbon sources. Protein expression was induced by addition of isopropyl-1-thio-β-galactopyranoside to a final concentration of 1 mM. After induction, the cells were cultured at 25°C over night and were lysed. The GST-fused Atg8 K26P was purified using a glutathione-Sepharose 4B column (GE Healthcare), and GST was excised from the Atg8 K26P with PreScission protease (GE Healthcare). Then, the excised GST and PreScission protease were removed from Atg8 K26P on a glutathione-Sepharose 4B column. Atg8 K26P was further purified using a CM cation exchange column (GE Healthcare) followed by a Superdex75 gel filtration column (GE Healthcare). Finally, Atg8 K26P was concentrated using a Centriprep 10 K ultra filtration system (Millipore) and then applied to NMR experiments.

NMR measurements and structure calculation

NMR experiments were carried out at 25°C on Varian UNITY INOVA 800 and 600 spectrometers. Measurements for structural analysis were made using a protein of 0.6 mM in 20 mM phosphate buffer (pH 6.8) and 150 mM NaCl in the presence of 1 mM DTT. Two- and three-dimensional NMR spectra were processed using the NMRPipe program (Delaglio et al. 1995) and the data analysis was performed with the help of the Sparky program (Goddard and Kneller 1997). ^{1}H, ^{13}C and ^{15}N resonance assignments were carried out using the following set of spectra; [^{1}H-^{15}N] HSQC, [^{1}H-^{13}C] HSQC, HNCO, HN(CO)CA, HNCA, HBHA (CO)NH, HN(CA)HA, C(CO)NH, HC(C)H-TOCSY, (H)CCH-TOCSY, HbCbCgCdHd, and HbCbCgCdCeHe. The ^{1}H, ^{13}C and ^{15}N chemical shifts were referenced to DSS according to IUPAC recommendations. Interproton distance restraints for structural calculation were obtained from ^{13}C-edited NOESY-HSQC and ^{15}N-edited NOESY-HSQC spectra using a 100 ms mixing time. The structure was calculated using the CYANA 2.1 software package (Herrmann et al. 2002). As an input for the final calculation of the three-dimensional structure of the Atg8 K26P, a total of 2,314 distance and 155 dihedral angle restraints predicted by TALOS program (Cornilescu et al. 1999) was used (Table 1). At each stage, 100 structures were calculated using 30,000 steps of simulated annealing, and a final ensemble of 20 structures was selected based on CYANA target function values. The atomic coordinates have been deposited in the Protein Data Bank (PDB code:2kwc).

Results and discussion

Based on the sequence alignment of Atg8 with the structure-reported homologues (GABARAP, GATE-16, LC3, and TbAtg8), a Pro residue was found to be conserved among the homologues but was occupied by a Lys residue (Lys26) in Atg8 (Fig 1). Thus we prepared Atg8 K26P. To

examine the effect of K26P substitution on the lipidation of Atg8, we performed in vitro conjugation assay (Fig. 2A) and detected the accumulation level of Atg8-PE in vivo by western blotting (Fig. 2B, lower panels). Further to examine the effect of this mutation on autophagic activity, we also studied the Ape1 maturation by western blotting (Fig. 2B, upper panels), and performed the alkaline phosphatase (ALP) assay (Fig. 2C). These results showed that the Atg8 K26P mutant undergoes lipidation and has an autophagic activity similar to that of the wild type. Therefore, Atg8 K26P can be used as an active mutant.

Table 1 Structural statistics of the Atg8 K26P

NOE distance constraints	2,314
Short range (intraresidue and sequential)	2,109
Medium range ($2 \leq \|i - j\| \leq 4$)	394
Long range ($\|i - j\| > 4$)	567
TALOS angle constrains (ϕ and φ)	155
Number of violations	
Distance > 0.2 Å	0
Angle > 5°	0
Structural coordinates rmsd (Å) (range 11–110)	
Backbone atoms	0.48
All heavy atoms	0.97
Ramachandran plot	
Most favored regions	78.8%
Additionally allowed regions	21.2%
Generously allowed regions	0.0%
Disallowed regions	0.0%

Atg8 K26P showed much improvement in the quality of the NMR spectra (Fig. 2D–F) along with increase in the sample stability from 1 week to over a month at 25°C. The residues with much higher intensity in the [^{1}H-^{15}N] HSQC spectrum of Atg8 K26P compared to the wild type were located on the α2-helix (Fig. 2E, F). Since the substituted Pro residue is located at the hinge region between the N-terminal α-helix domain and the ubiquitin-like domain, the relative arrangement of the α2-helix to the ubiquitin-like domain in Atg8 K26P seems to be more fixed, suggesting that the N-terminal α-helix domain in the wild type is in equilibrium between the open and closed conformations. This view is supported by the evidence that the complex of Atg8 and an Atg19 peptide is stable in NMR conditions over a month (Noda et al. 2008), where the aromatic side chain of Atg19 Trp412 was deeply stuck into the hydrophobic pocket formed by the N-terminal α-helix domain and the C-terminal ubiquitin-like domain. This hydrophobic interaction might restrict the mobility of the α2-helix. This is consistent with the evidence that the broad

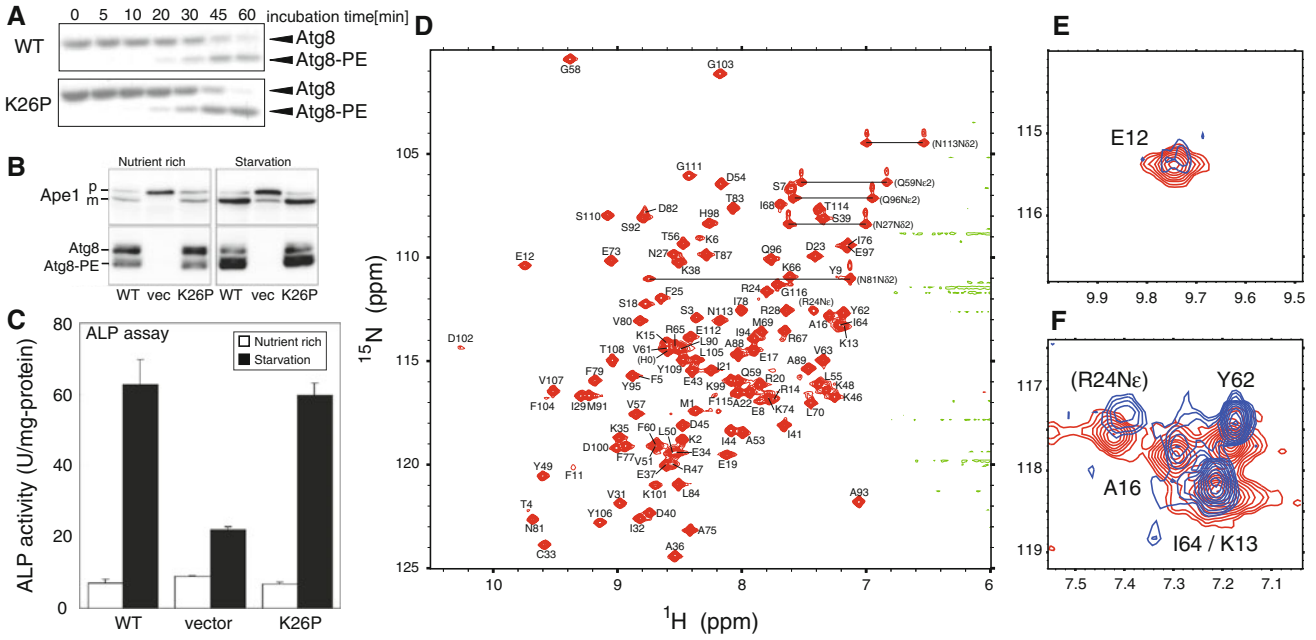

Fig. 2 The comparison of the autophagic activities and the [^{1}H-^{15}N] HSQC spectra between the Atg8 wild type and the K26P mutant. **A** In vitro conjugation assay (Ichimura et al. 2004). The wild type and the K26P mutant were conjugated to PE in a similar efficiency. **B** In vivo autophagic activity assay. The vacuolar transport of Ape1 was assessed by detecting the cleavage of its propeptide by western blotting (*upper panel*). The accumulation level of Atg8-PE in vivo was detected by western blotting (*lower panel*). **C** In vivo autophagic activity by the ALP assay. Cells were grown in nutrient rich conditions (*white bars*) and then starved in nutrient deficient conditions for 4.5 h to induce autophagy (*black bars*), and their autophagic activities were examined by the ALP assay (Noda et al. 1995). **D** The [^{1}H-^{15}N] HSQC spectra of Atg8 K26P in red with the assignment. **E** and **F** show the portion of the [^{1}H-^{15}N] HSQC spectra of Atg8 K26P, focusing on the signals of Glu12 and Ala16 (the wild type in *blue* and the K26P mutant in *red*), respectively

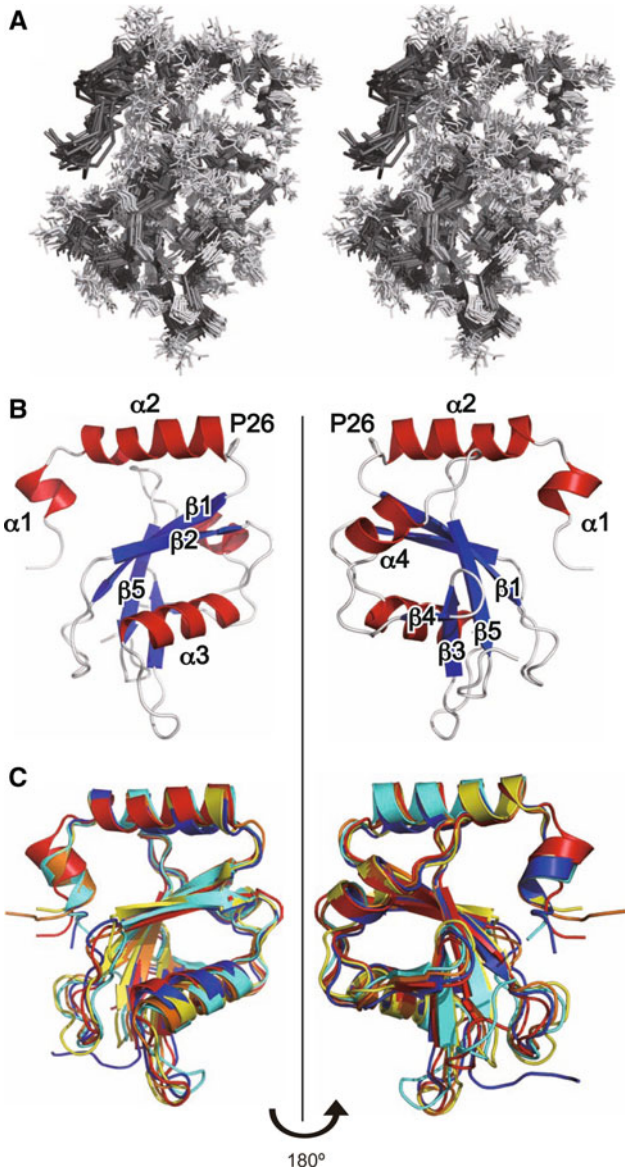

Fig. 3 Structures of Atg8 K26P. **A** Overlay of the ensemble of 20 final energy-minimized CYANA structures in stereo. The main and side chains are shown in *black* and *light gray*, respectively. **B** Ribbon diagrams of the lowest energy structure. Pro26 residue is shown in a stick model. **C** Overlay of Atg8 K26P (*red*), GABARAP (*cyan*, PDB code: 1GNU), GATE-16 (*green*, PDB code: 1EO6), LC3 (*yellow*, PDB code: 1UGM), TbAtg8 (*blue*, PDB code: 3H9D), and Atg8-Atg19 peptide complex (*orange*, PDB code: 2ZPN). The structures were drawn using PyMOL [http://www.pymol.org/]

peaks assigned to the N-terminal α-helix domain in the wild type become similarly sharpened on the addition of Atg19 peptide (data not shown).

The resonance assignments of Atg8 K26P has been almost completed except for the Arg14 side-chain (Cβ–Cδ, Hβ–Hδ) and several aromatic side chains (Cε1, Cε2, Hε1, and Hε2 of Phe5, Cζ and Hζ of Phe11). The structure of Atg8 K26P was calculated using the CYANA 2.1 software package (Herrmann et al. 2002) based on the interproton distance restraints and dihedral angle restraints. The overlay of the 20 structures and the ribbon model of the lowest energy structure are shown in Fig. 3A, B. The α1 helix region has lower structural convergence than the α2-helix and the ubiquitin-like domain, because of the small number of NOE signals around this region. The overall structure of Atg8 K26P is similar to those of Atg8 complexed with the Atg19 peptide (Noda et al. 2008) and the Atg8 homologues (Fig. 3C), being comprised of the N-terminal α-helix domain containing two α-helices (α1; 4–9, α2; 11–25) and the C-terminal ubiquitin-like domain.

We have constructed an Atg8 mutant that is stable in NMR sample conditions and determined the structure at the ligand-free state. This mutant has similar biological activities comparable to that of the wild type. Atg8 is suggested to be in two conformations, the open and the closed forms from the in vitro biological assays (Nakatogawa et al. 2007). We considered that the structure of the K26P mutant corresponds to the closed conformation. Further studies including relaxation-dispersion and hydrogen-exchange studies are required to reveal the conformational equilibrium between the open and the closed conformations.

References

Bavro VN, Sola M, Bracher A, Kneussel M, Betz H, Weissenhorn W (2002) Crystal structure of the GABA(A)-receptor-associated protein, GABARAP. EMBO Rep. 3:183–189

Cornilescu G, Delaglio F, Bax A (1999) Protein backbone angle restraints from searching a database for chemical shift and sequence homology. J Biomol NMR 13:289–302

Delaglio F, Grzesiek S, Vuister GW, Zhu G, Pfeifer J, Bax A (1995) NMRPipe: a multidimensional spectral processing system based on unix pipes. J Biomol NMR 6:277–293

Goddard TD, Kneller DG (1997) SPARKY 3, University of California, San Francisco. http://www.cgl.ucsf.edu/home/sparky/

Herrmann T, Güntert P, Wüthrich K (2002) Protein NMR structure determination with automated NOE assignment using the new software CANDID and the torsion angle dynamics algorithm DYANA. J Mol Biol 319:209–227

Ichimura Y, Imamura Y, Emoto K, Umeda M, Noda T, Ohsumi Y (2004) In vivo and in vitro reconstitution of Atg8 conjugation essential for autophagy. J Biol Chem 279:40584–40592

Kirisako T, Ichimura Y, Okada H, Kabeya Y, Muzushima N, Yoshimori T, Ohsumi M, Takao T, Noda T, Ohsumi Y (2000) The reversible modification regulates the membrane-binding state of Apg8/Aut7 essential for autophagy and the cytoplasm to vacuole targeting pathway. J Cell Biol 151:263–276

Koopmann R, Muhammad K, Perbandt M, Betzel C, Duszenko M (2009) Trypanosoma brucei ATG8: Structural insights into autophagic-like mechanisms in protozoa. Autophgy 5:1085–1091

Mizushima N (2007) Autophagy: process and function. Genes Dev 21:2861–2873

Nakatogawa H, Ichimura Y, Ohsumi Y (2007) Atg8, a ubiquitin-like protein required for autophagosome formation, mediates membrane tethering and hemifusion. Cell 130:165–178

Nakatogawa H, Suzuki K, Kamada Y, Ohsumi Y (2009) Dynamics and diversity in autophagy mechanisms: lessons from yeast. Nat Rev Mol Cell Biol 10:458–467

Noda T, Matsuura A, Wada Y, Ohsumi Y (1995) Novel system for monitoring autophagy in the yeast *Saccharomyces cerevisiae*. Biochem Biophys Res Commun 210:126–132

Noda NN, Kumeta H, Nakatogawa H, Satoo K, Adachi W, Ishii J, Fujioka Y, Ohsumi Y, Inagaki F (2008) Structural basis of target recognition by Atg8/LC3 during selective autophagy. Genes Cells 13:1211–1218

Noda NN, Ohsumi Y, Inagaki F (2009) ATG systems from the protein structural point of view. Chem Rev 109:1587–1598

Paz Y, Elazar Z, Fass D (2000) Structure of GATE-16, membrane transport modulator and mammalian ortholog of auphagocytosis factor Aut7p. J Biol Chem 275:25445–25450

Schwarten M, Stoldt M, Mohrlüder J, Willbold D (2009) Sequence-specific ^{1}H, ^{13}C, and ^{15}N resonance assignment of the autophagy-related protein Atg8. Biomol NMR Assign 3:137–139

Stangler T, Mayr LM, Willbold D (2002) Solution structure of human GABA(A) receptor-associated protein GABARAP: implications for biological function and its regulation. J Biol Chem 277:13363–13366

Sugawara K, Suzuki NN, Fujioka Y, Mizushima N, Ohsumi Y, Inagaki F (2004) The crystal structure of microtubule-associated protein light chain 3, a mammalian homologue of *Saccharomyces cerevisiae* Atg8. Genes Cells 9:611–618

Yamada Y, Suzuki NN, Hanada T, Ichimura Y, Kumeta H, Fujioka Y, Ohsumi Y, Inagaki F (2007) The crystal structure of Atg3, an autophagy-related ubiquitin carrier protein (E2) enzyme that mediates Atg8 lipidation. J Biol Chem 282:8036–8043